

# 5-Endo cyclizations of NHC-boraallyl radicals bearing ester substituents. Characterization of derived 1,2-oxaborole radicals and boralactones

Wen Dai,<sup>‡</sup> Timothy R. McFadden,<sup>‡</sup> Dennis P. Curran,<sup>\*‡</sup> Herbert A. Früchtl<sup>†</sup> and John C. Walton<sup>\*†</sup>

<sup>‡</sup> Department of Chemistry, University of Pittsburgh, Pittsburgh, Pennsylvania 15260, United States.

<sup>†</sup> EaStCHEM School of Chemistry, University of St. Andrews, St. Andrews, Fife, KY16 9ST, United Kingdom.

**ABSTRACT:** EPR studies of radical hydrogen abstraction reactions of N-heterocyclic carbene (NHC) complexes of alkenylboranes bearing two ester substituents revealed not the expected boraallyl radicals but instead isomeric 1,2-oxaborole radicals. Such radicals are new, and DFT calculations show that they arise from the initially formed boraallyl radicals by a rapid, exothermic 5-*endo* cyclization. These spectroscopic and computational discoveries prompted a series of preparative experiments that provided access to a novel family of robust NHC-boralactones. A one-pot procedure was developed to access the boralactones directly from an NHC-borane (NHC-BH<sub>3</sub>) and dimethyl acetylene dicarboxylate.

## Introduction

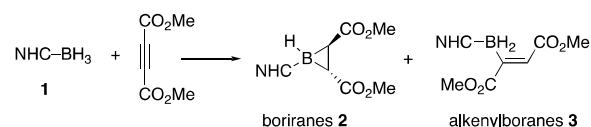
N-Heterocyclic carbene boranes (NHC-boranes)<sup>1</sup> are robust complexes that have proved to be versatile reagents for new radical,<sup>2</sup> ionic,<sup>3</sup> and organometallic reactions.<sup>4</sup> The B–H bonds of NHC-boranes are 12–20 kcal/mol weaker than those of uncomplexed boranes,<sup>2c,5</sup> and this property is at the root of much of their versatility. The reactivity of NHC-boranes can be tuned by employing NHCs with differing Lewis base strength.<sup>6</sup> The extent of steric shielding of the B–H bonds by substituents on the N-atoms of the ligands also significantly influences reactivity and selectivity.

The parent NHC-boryl radicals (NHC–BH<sub>2</sub>•) are key intermediates in small molecule and polymer synthesis<sup>2</sup> and have been characterized by electron paramagnetic resonance (EPR) spectroscopy and calculations.<sup>2c,7</sup> Much less is known about B-substituted NHC-boryl radicals. Hydrogen atom abstraction from B-aryl boranes (NHC–BH<sub>2</sub>–Ar) by *tert*-butoxyl radicals (*t*-BuO•) occurs at boron and produces distinctive NHC–B•(H)–Ar radicals.<sup>8</sup> The spin in these radicals is delocalized into the aryl rings such that they amount to  $\alpha$ -borabenzyl radicals. Related diaryl radicals with bulky aryl groups NHC–B(Ar<sub>2</sub>)• are persistent and loosely resemble trityl radicals.<sup>9</sup>

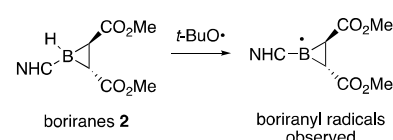
Recently, we discovered a direct synthetic route to both boriranes **2** and alkenylboranes **3** by hydroboration reactions of acetylenedicarboxylate esters and NHC-boranes **1** (Figure 1a).<sup>10</sup> The NHC-boriranes **2** undergo H-abstraction reactions with *tert*-butoxyl radical to form novel NHC-boriranyl radicals (Figure 1b).<sup>11</sup>

In line with these studies, we hypothesized that *tert*-butoxyl radicals would rapidly abstract H-atoms from the BH<sub>2</sub> groups of NHC-alkenylboranes **3**, thus generating hitherto unknown 1-boraallyl radicals **4**. However, in the event, surprising chemistry was uncovered; the expected B-centered radicals **4** were never observed by EPR spectroscopy because they undergo rapid 5-*endo* ring closures onto one of the ester carbonyl O-atoms to form unusual 1,2-oxaborole radicals **5** (Figure 1c). This paper describes the discovery and characterization of the intermediate 1,2-oxaborole radicals **5**. These EPR and computational studies in turn engendered a preparative method to form rare unsaturated boralactone derivatives.

(a) double hydroboration reaction, ref. 10



(b) generation of boriranyl radicals, ref. 11



(c) unexpected formation of 1,2-oxaborole radicals, this work

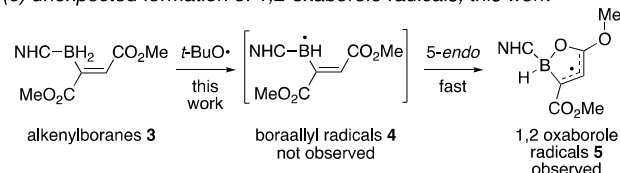


**Figure 1.** Synthesis of NHC-boriranes and NHC-alkenylboranes and radical forming reactions

## Results and Discussion

### Preparation of Alkenylboranes.

The structures of all the (*E*)-alkenylboranes involved in this study are shown in Figure 2. EPR studies focused on the boranes **3a–c**, which have identical N-substituents and therefore should exhibit simpler spectra. These are imidazol-2-ylidene boranes with dimethyl (**3a**), diisopropyl (**3b**) and bis-2,6-diisopropylphenyl (dipp, **3c**) substituents. The diphenyl analog **3d** served as a computational model of **3c**. Preparative reactions were conducted with **3a** and **3b**, and additionally with unsymmetrical imidazol-2-ylidenes **3e** (*i*-Pr and Me), **3f** (Bu and Me) and **3g** (Bn and Me) and with the benzimidazol-2-ylidene analog **3h**.

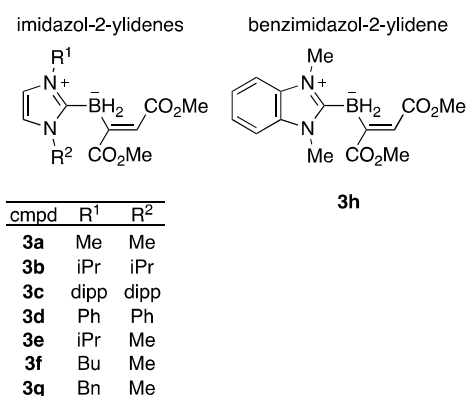
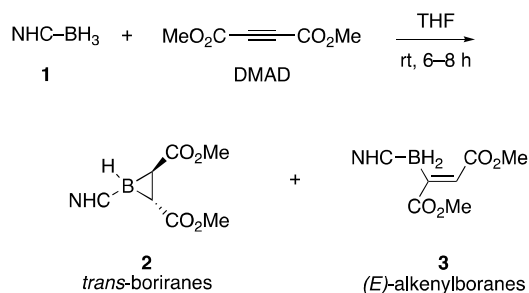


**Figure 2.** Structures of (*E*)-alkenylboranes used in this study (dipp is 2,6-diisopropylphenyl)

A sample of the bis-dipp NHC-borane **3c** was already available from the prior work.<sup>10</sup> Scheme 1 and Table 2 summarize how all the other alkenylboranes were made. In the standard procedure (Scheme 1), a THF solution of dimethyl acetylenedicarboxylate (DMAD, 2 equiv) was added dropwise to a THF solution of the starting borane **1**, then the resulting solution was stirred for 6–8 h at rt. Concentration and flash chromatography provided the target (*E*)-alkenylboranes **3** (less polar) along with the isomeric boriranes **2** (more polar). This new procedure is a modification of the original one<sup>10</sup> that is simpler (cryogenic cooling is no longer needed) and typically provides better yields.

### Scheme 1. Synthesis of (*E*)-alkenylboranes 3



As Table 1 shows, this series of experiments gave rather consistent results. Isolated yields of the various (*E*)-alkenyl boranes **3** ranged from 25–36% while the isomeric *trans*-boriranes **2** were isolated in 23–28% yields. Combined yields of both products ranged from 49–60%. The alkenylboranes **3** were isolated as pure (*E*)-isomers and the boriranes **2** were exclusively *trans*. The ratios of the isolated alkenylborane/borirane products are rather close to 1/1 (except for **3a/2a**, which is about 3/2). The pairs **2a/3a** and **2b/3b** are known compounds.<sup>10</sup> All the other compounds in Table 1 are new and have been fully characterized (see Supporting Information). Going forward, we focus on radical transformations of the (*E*)-alkenylboranes **3**, though the boriranes **2** are also being used for other kinds of experiments.

**Table 1.** Preparation of (*E*)-alkenylborane precursors<sup>a</sup>

entry	borirane, yield <sup>b</sup>	alkenylborane, yield <sup>b</sup>
1	<b>2a</b> , 23% 	<b>3a</b> , 36% 
2	<b>2b</b> , 23% 	<b>3b</b> , 26% 
3	<b>2e</b> , 26% 	<b>3e</b> , 27% 
4	<b>2f</b> , 28% 	<b>3f</b> , 32% 
5	<b>2g</b> , 24% 	<b>3g</b> , 25% 
6	<b>2h</b> , 24% 	<b>3h</b> , 28% 

a) 1 equiv **1**, 2 equiv DMAD, THF, rt, 6–8 h; b) isolated yields after purification by flash chromatography

### EPR Spectroscopic Study of H-atom Abstraction.

Dispersions of each NHC-alkenylborane (**3a–c**) and di-*tert*-butyl peroxide (DTBP) were prepared in *tert*-butylbenzene, sonicated and deaerated by bubbling N<sub>2</sub> for 10 min. Individual samples (0.2 mL) in quartz tubes were irradiated in the resonant cavity of the EPR spectrometer with unfiltered UV light from a 500 W high pressure mercury arc lamp. Solubility restricted the accessible temperature range; but a strong spectrum of a single radical was obtained from 240 to 300 K for each sample. The spectrum from **3c** at 260 K is representative and is shown in Figure 3a. This spectrum persisted for several seconds on shuttering the UV light. Figure 3b shows the simulated spectrum, which was computed with the hyperfine coupling constants listed in Table 2.

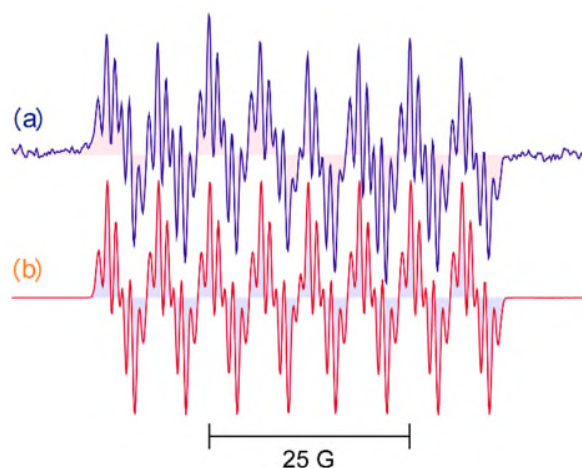


**Figure 3.** CW EPR spectrum during UV irradiation of **3c** in PhBu-t at 260 K. (a) Experimental. (b) Computer simulation.

**Table 2.** EPR Parameters for Radicals Derived from Alkenylboranes **3a–c**<sup>a</sup>

Precursor	R	expt or DFT <sup>b</sup>	<i>g</i> -factor	<i>a</i> ( <sup>11</sup> B)	<i>a</i> (H)	<i>a</i> (H <sup>v</sup> )	<i>a</i> (2N)	<i>a</i> (other)
<b>3a</b>	Me	expt at 240 K	2.0033	6.01	26.01	1.64	–	1.12 (3H); 0.50 (3H)
	Me	DFT of <b>4a</b>		6.96	–11.08	–7.45	2.3	1.9 (6H)
	Me	DFT of <b>5a</b>		–5.87	25.51	–1.4	<0.5	1.50 (3H); 1.20 (3H)
<b>3b</b>	<i>i</i> -Pr	expt at 240 K	2.0033	6.65	26.57	1.65	–	1.05 (3H); 0.62 (3H)
	<i>i</i> -Pr	DFT of <b>4b</b>		7.09	–9.92	–10.98	1.8	–
	<i>i</i> -Pr	DFT of <b>5b</b>		–5.94	25.82	–1.73	<0.5	1.52 (3H); 1.25 (3H)
<b>3c</b>	dipp	expt at 260 K	2.0032	6.38	24.97	1.74	–	1.03 (3H)
	dipp	DFT <sup>c</sup> of <b>4c</b>		6.74	–11.01	–6.72	2.0	1.0 (2H)
	dipp	DFT of <b>5c</b>		–5.75	24.46	–1.86	<0.5	1.54 (3H); 1.28 (3H)

<sup>a</sup> Hfs in Gauss (G); note that EPR gives only the magnitude, not the sign of hfs. <sup>b</sup> DFT method: B3LYP/epr-iii//B3LYP/6-31+G(d).

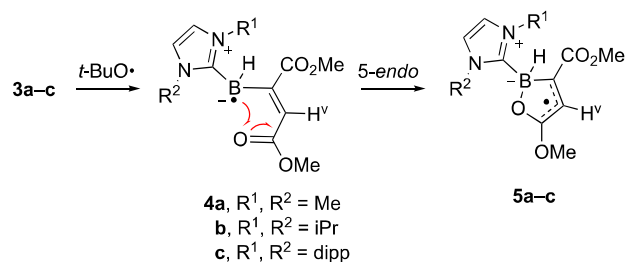
<sup>c</sup> B3LYP/epr-ii (epr-iii failed).

We anticipated that the *t*-BuO• radicals, generated from the DTBP, would abstract comparatively weakly bound (B)–H atoms with production of boraallyl radicals **4** (Scheme 2). However, such boraallyl radicals are expected to show sizeable hfs from the allyl H-atom (H<sup>v</sup>) as well as hfs from the N-atoms of the NHC rings.<sup>7–9,11</sup> DFT computations (B3LYP/epr-iii)<sup>12</sup> confirmed this expectation for each potential boraallyl radical (**4a–c**) (see Table 2). The matches between experimental hfs and computed hfs were poor across the board, so we concluded that the observed species were not boraallyl radicals.

**Scheme 2.** Generation and 5-*endo* ring closure of NHC-ligated boraallyl radicals.

Somewhat similar spectra were obtained from photolyses of DTBP with **3a** and **3b** (see Figures S1 to S4 in the Supporting Information) except the signals did not persist when the light was shuttered. When thermolysis of 2,2'-azobis(2-methylpropionitrile) (AIBN) was used as initiator in place of the DTBP, only the initiator-derived 2-cyanopropyl radical was observed; even at T = 340 K (Supporting Information Figure S6). Thus, this C-centered radical was less efficient than the O-centered *t*-butoxyl radical at abstracting H-atoms. This result does not, of course, preclude H-abstraction by 2-cyanopropyl radicals at the higher temperatures of the preparative experiments (see below).

Table 2 summarizes all the EPR parameters obtained in this work, both experimental and calculated. The experimental spectra all show one large hyperfine splitting (hfs) from a single H-atom (25–26 G), a moderate hfs from a B-atom (about 6 G) and several small hfs from other H-atoms. No hfs attributable to the N-atoms of NHC rings were resolved.



Still, it seems likely that boraallyl radicals should be the primary products of H-atom abstraction, so we searched for secondary reactions. During a DFT scan starting from boraallyl radical **4b**, we found that the structure finally optimized to a global minimum structure that was a 5-member oxaborole radical **5b** (Scheme 2).

We next carried out DFT potential energy scans with **4a–c**, varying all flexible dihedral angles in steps of 45° and optimizing the geometry from the resulting starting structure. Again,

the lowest energy structures were 5-member oxaborole rings **5**.

The computed EPR parameters for oxaborole radicals **5a–c** were in good agreement with the hfs of the spectroscopically observed species (see Table 2). We therefore conclude that radicals **4 a–c** are generated under these conditions but that they undergo rapid ring closure to oxaborole radicals **5a–c** even at 240 K.

The DFT-computed structures of **4a** and **5a** are illustrated in Figure 4. Radical **4a** is a typical NHC-boryl radical<sup>2c,7,8</sup> with a roughly planar boron atom, oriented to allow delocalization of the spin into the NHC ring. However, the B–alkenyl bond is twisted to reduce A<sup>1,3</sup>-strain, so radical **4a** does not benefit much from allylic stabilization. The oxaborole radical **5a** is roughly planar, allowing delocalization of the spin throughout the heterocycle and its substituents (OMe and CO<sub>2</sub>Me).

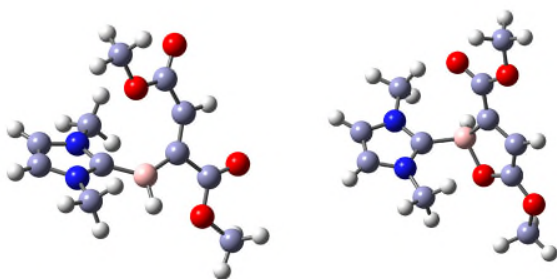


**Figure 4.** DFT-computed structures of boraallyl radical **4a** (left) and oxaborole radical **5a** (right).

The formation of **5** was unexpected because 5-*endo* radical cyclizations are disfavored and examples are sparse.<sup>13</sup> Moreover, radical cyclizations onto the O-atoms of carbonyl groups are even more unusual.<sup>14</sup> To the best of our knowledge, these are the first examples of 5-*endo* cyclizations of boryl radicals.

#### DFT Study of the Scope of the 5-*endo* Ring Closure.

A set of five assorted NHC-boryl radicals with pendant carbonyl-containing arms was chosen for DFT study (Figure 5). The NHC ring in all the computed structures is 1,3-dimethylimidazol-2-ylidene. The reaction enthalpies and free energies ( $\Delta H^0$ ,  $\Delta G^0$ ) for the 5-*endo* cyclizations as well as the activation enthalpies and free activation energies ( $\Delta H^\ddagger$ ,  $\Delta G^\ddagger$ ) were computed with the UB3LYP/6-311+G(2d,p) method and with CPCM solvent continuum model and toluene as solvent. The resulting values are shown in Figure 5.

In agreement with the EPR experimental results, the 5-*endo* ring closure of boraallyl radical **4a** onto the carbonyl O-atom was found to be exothermic (–13.3 kcal/mol) and to have a small activation barrier (4.1 kcal/mol). An important factor favoring the ring closure is the thermodynamic stabilization resulting from the allyl-type delocalization in the product oxaborole radical **5a**.

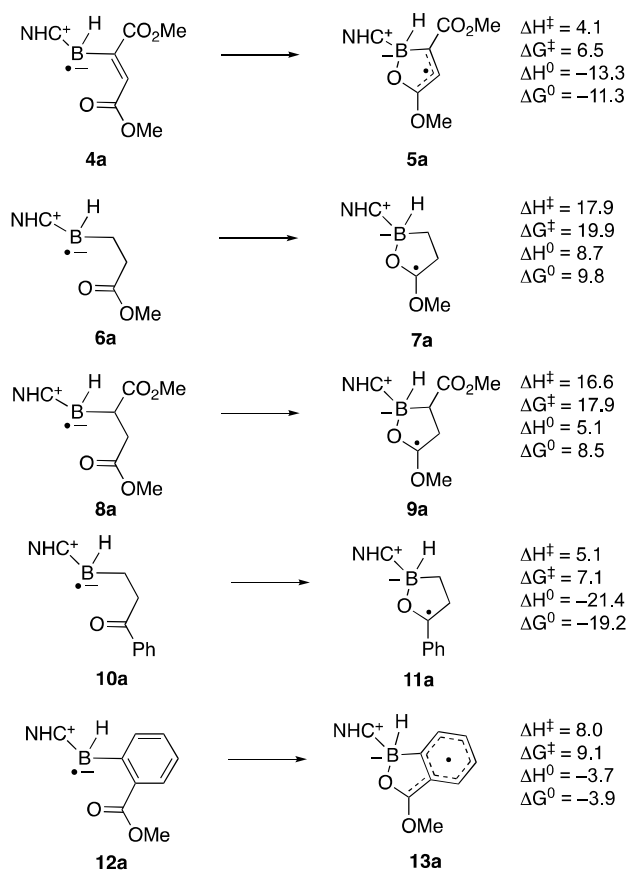


**Figure 5.** DFT Energetics for 5-*endo* ring closures of NHC-boryl radicals (energies in kcal/mol). NHC is 1,3-dimethylimidazol-2-ylidene

Precursor NHC-boryl radical **6a** lacks the alkene in **4a** and forms an oxaborole radical **7a** with no allylic stabilization. Indeed, ring closure was endothermic (by 8.7 kcal/mol) and had a high barrier (17.9 kcal/mol). The ring closure of B-centered radical **8a**, having both ester groups of **4a** but again lacking the alkene, was also computed. The oxaborole radical **9a** again lacks stabilization, and this reaction was also endothermic. However, when benzyl-type stabilization was present in the ring-closed oxaborole radicals, either as in **11a** or **13a**, ring closures of the corresponding radicals **10a** and **12a** were exothermic and had low barriers.

These preliminary calculations support the rapid cyclization of radicals **4** to the ester oxygen and show that the alkene is a crucial element in lowering the energy barrier. They further suggest that other cyclizations of NHC-boryl radicals to carbonyl groups might be observable if the product radicals are stable enough.

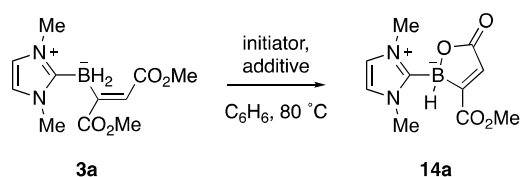
#### Preparative Reactions of (*E*)-Alkenylboranes.

With the goal to identify stable products resulting from these new 5-*endo* cyclizations, we next conducted preparative reactions of (*E*)-alkenylboranes. Here we switched from low temperature photochemical to thermal methods for radical generation, and the results of several key pilot experiments are

shown in Table 3. These reactions were conducted in sealed vessels with air atmosphere.

First, reaction of (*E*)-alkenylborane **3a** with 50 mol% DTBP at 80 °C was slow and gave only some decomposition (entry 1). Instead of increasing the temperature to favor the homolysis of DTBP, we conducted a similar thermal experiment with 50% AIBN (entry 2, 80 °C, 12 h). This produced a robust new product whose <sup>11</sup>B NMR yield was estimated at 50% based on the broad doublet at −5.7 ppm (*J*<sub>BH</sub> = 105 Hz). The new product was isolated in 38% yield by flash chromatography and was soon identified as a 5*H*-1,2λ<sup>2</sup>-oxaborol-5-one **14a**, hereafter called a boralactone. The resonance in the <sup>11</sup>B NMR spectrum is in a region typical for NHC-boranes with B–O bonds. In the <sup>13</sup>C NMR spectrum, **14a** exhibits two carbonyl carbon resonances (177.4 and 168.2 ppm) but only one methyl ester resonance (51.6 ppm).

**Table 3. Synthesis of a new boralactone 14a**



entry	initiator <sup>a</sup>	additive	<sup>11</sup> B NMR yield <b>14a</b>	isolated yield <b>14a</b>
1	DTBP	–	0%	–
2	AIBN	–	50%	38%
3	AIBN	Bu <sub>3</sub> SnH, 50%	78%	59%
4	–	Bu <sub>3</sub> SnH, 50%	0%	–
5	AIBN	Bu <sub>3</sub> SnH, 100%	84%	58%
6 <sup>b</sup>	AIBN	Bu <sub>3</sub> SnH, 50%	71%	62%

a) 50 mol%, b) solvent is C<sub>6</sub>H<sub>5</sub>CF<sub>3</sub> (BTF)

Boralactones are a little known class of molecules that result from (formal) nuclear substitution of carbon by boron in a standard lactone. Most known boralactones are cyclic ester derivatives of boronic acids.<sup>15,16</sup> In contrast, **14a** is a ligated boronic acid lactone. Ligated boralactones of any kind are especially rare and the extant examples are only distantly related to **14a**.<sup>17</sup>

We also found that addition of 50% AIBN and 50% tributyltin hydride (Bu<sub>3</sub>SnH) to **3a** increased both the NMR yield (from 50% to 78%) and the isolated yield (from 38% to 59%) of boralactone **14a** (Table 3, entry 3). No reaction occurred when Bu<sub>3</sub>SnH was added and AIBN was omitted (entry 4), so AIBN is the more important of the two additives. Increasing the amount of Bu<sub>3</sub>SnH to 100% (entry 5) gave a slightly better NMR yield of **14a** (84%), but about the same isolated yield (58%). Finally, a reaction of **3a** in benzotrifluoride (entry 6, C<sub>6</sub>H<sub>5</sub>CF<sub>3</sub>, 50% AIBN and 50% Bu<sub>3</sub>SnH) gave yields comparable to the benzene experiment (71%, NMR; 62%, isolated).

These reaction conditions suggest a radical mechanism; however, we considered that boralactone **14a** could also be formed by an ionic mechanism if an electrophilic boron species were somehow generated. However, no boralactone **14a** was produced when **3a** was treated with three reagents that

are commonly used to make electrophilic NHC-boreonium species (NBS, Ph<sub>3</sub>CBF<sub>4</sub> and TfOH).<sup>18</sup>

We next conducted preparative reactions of the other alkenylboranes under a standard set of conditions (50 mol% AIBN, 50 mol% Bu<sub>3</sub>SnH, benzene, 80 °C, 6 h, air atmosphere). Concentration and flash chromatography provided the corresponding boralactones **14b**, and **14e–14h**, as shown in Figure 6. The isolated yields ranged from 57–65%. All these boralactones were robust compounds that were fully characterized.

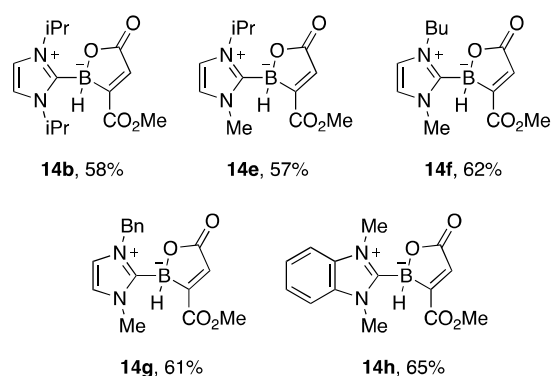
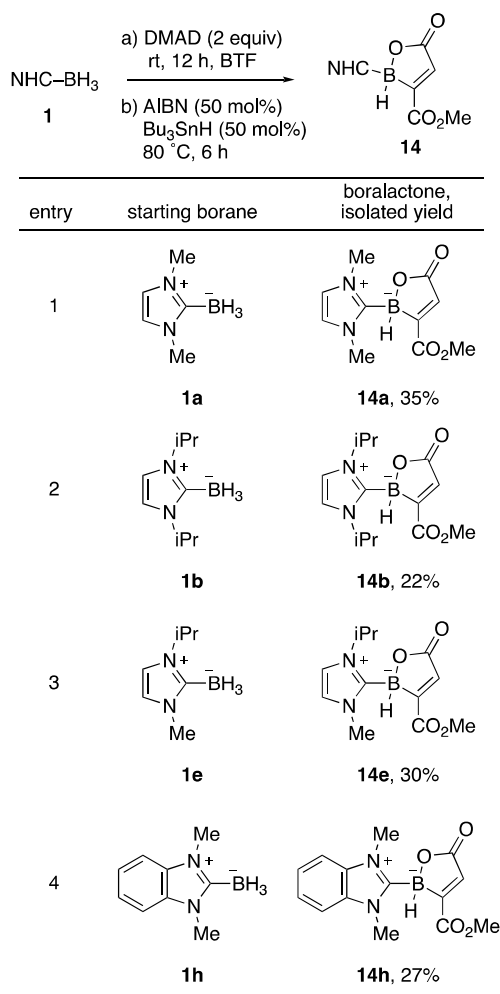


**Figure 6.** Structures and isolated yields of boralactones derived from the corresponding (*E*)-alkenylboranes (reaction conditions: 50 mol% AIBN, 50 mol% Bu<sub>3</sub>SnH, benzene, 80 °C, 6 h)

We also studied a one-pot procedure to make boralactones directly from the unsubstituted NHC-boranes **14** and DMAD (see Scheme 1), bypassing the isolation of the (*E*)-alkenylboranes **3**. The results of four preparative experiments are shown in Table 4. In the standard procedure, a BTF solution of DMAD was added dropwise over a few minutes to the starting NHC-borane **1** (also in BTF). After 12 h, AIBN and Bu<sub>3</sub>SnH (both 50 mol%) were added and the mixture was heated at 80 °C for 6 h. Cooling, concentration and flash chromatography provided the corresponding boralactones **14** in 22–35% yield (based on the starting NHC-borane **1**).

This procedure to make boralactones **14** is more convenient than the two-step method, and the isolated yields are typically better. For example, the two-step yield of boralactone **14a** is 23% (as derived from the yields of Table 3 (59%) and entry 1 in Table 1 (39%)), while the one-pot yield is 35% (Table 4, entry 1). Boriranes **2** are of course also formed in the first stage of these one-pot reactions (see Table 1), but they are largely inert to the conditions of the second stage and are readily separable from the target boralactones.

**Table 4. Direct (one-pot) Synthesis of Boralactones from NHC-boranes and DMAD**



### Mechanism of Boralactone Formation.

To conclude the study, we conducted experiments and calculations to address the mechanism of boralactone formation, and we considered the two general paths shown in Figure 7. In the radical path, cyclization of boraallyl radical **4** to oxaborole radical **5** is followed by a  $\beta$ -fragmentation reaction to give boralactone **14** and a methyl radical ( $\text{Me}\cdot$ ). In the oxidative path, the relatively electron rich oxaborole radical **5** is oxidized to an oxaborole cation **15** (or some equivalent species, see below), which in turn would transform to boralactone **14** by either hydrolysis or demethylation.

$\beta$ -Fragmentation is a major class of radical reactions, but it is not immediately clear that the radical path in Figure 7 is low in energy. Although a strong  $\text{C}=\text{O}$  bond is formed in the fragmentation (the boralactone carbonyl group), the starting oxaborole radical **5** is relatively stable while the product methyl radical is relatively unstable. We used DFT calculations to assess the likelihood of this reaction.

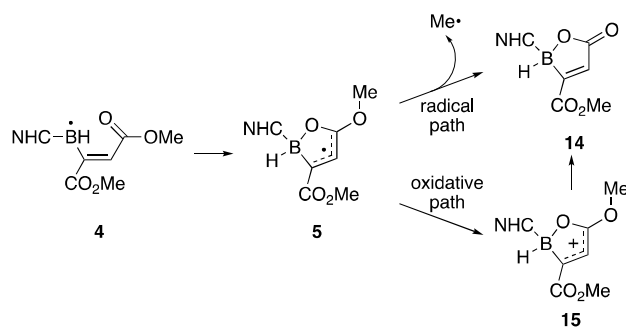


**Figure 7.** Possible radical and oxidative paths to boralactone **14**

The energetics of  $\beta$ -fragmentation of oxaborole radical **5a** were computed by using the DFT method described above (B3LYP/6-311+G(2d,p)) but including the CPCM continuum solvent model with toluene. These calculations indicate that the  $\beta$ -fragmentation to methyl radical is endothermic by 4.4 kcal/mol and has a high activation barrier ( $\Delta H^\ddagger$ ) of 22.0 kcal/mol (details in the Supporting Information). Based on these DFT calculations, we ruled out the radical path for formation of **14**.

Turning to the oxidative path, we considered both AIBN and dioxygen ( $\text{O}_2$ ) as possible oxidants. AIBN has been suggested to oxidize electron rich radicals,<sup>19</sup> whereas  $\text{O}_2$  is implicated because the preparative reactions are conducted in air. Control experiments quickly fingered  $\text{O}_2$  as the culprit. Specifically, several experiments with alkenylborane **4a** were conducted under  $\text{N}_2$  after degassing to remove residual  $\text{O}_2$  from air. The boralactone **14a** was not formed in any of these experiments. Thus, dioxygen, which is absent in the EPR experiments, is a critical component in the preparative experiments.

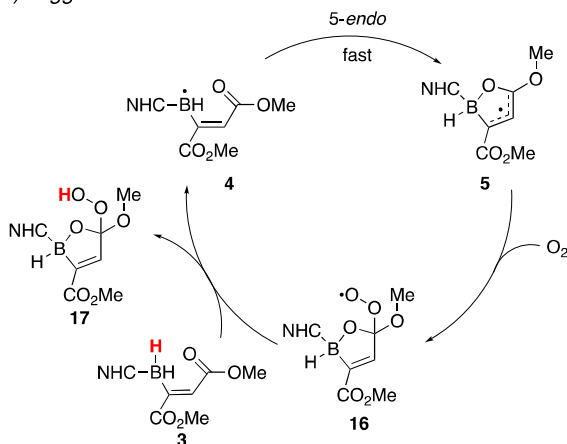
It is possible that dioxygen reacts with oxaborole radical **5** by an outer sphere electron transfer reaction<sup>20,21</sup> to directly give oxaborole cation **15** (Figure 7) and superoxide radical anion ( $\text{O}_2\cdot^-$ ). However, a net inner-sphere electron transfer path is perhaps more likely, and this is shown in the context of a suggested radical chain mechanism in Figure 8a.

Boraallyl radical **4** is formed in an initiation step and undergoes 5-*endo* cyclization to oxaborole radical **5**. This cyclization is fast (as shown by the EPR experiments) so the bimolecular reaction of **4** with oxygen cannot compete. Radical **5** then reacts with oxygen by combination<sup>21</sup> (rather than electron transfer) to provide allylic peroxy radical **16**.<sup>22</sup> In turn this radical abstracts hydrogen from the B-H bond of precursor **3** to provide peroxy orthoester **17** and the starting radical **4**. This reaction has precedent in the autoxidation of NHC-boranes (of the type  $\text{NHC-BH}_3$ ) and is a key step in allowing such boranes to mediate photopolymerizations in air.<sup>2b,23</sup>

This mechanism has the added advantage of providing plausible reasons for why the reaction works with AIBN alone but is improved by adding  $\text{Bu}_3\text{SnH}$ . With AIBN alone, the radical chain operates to provide peroxy orthoester **17**. This is an equivalent of oxaborole cation **15** and can be hydrolyzed to provide **14**. In the presence of  $\text{Bu}_3\text{SnH}$ , the conversion of **17** to **14** is improved because peroxy orthoester **17** can be reduced ionically by  $\text{Bu}_3\text{SnH}$  to hemi orthoester **18** and

Bu<sub>3</sub>SnOH (Figure 8b). In turn, hemi orthoester **18** will collapse rapidly to **14** and methanol. The ionic tin hydride reduction of peroxides formed under radical conditions is preceded by the work of Nakamura,<sup>24</sup> who observed that alkyl iodides are converted to alcohols (rather than alkanes) when their tin hydride reductions are conducted in air.

(a) suggested radical chain



(b) subsequent ionic reactions

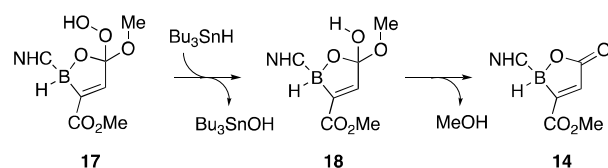


**Figure 8.** Plausible mechanism for boralactone formation

In the end, the EPR and preparative experiments both provide oxaborole radical **4** but then diverge from there. Under the EPR conditions (di-*t*-butyl peroxide, inert atmosphere), oxaborole radical **4** has no good path to closed-shell products (other than standard radical-radical termination reactions), making it easy to detect by EPR spectroscopy. Under the preparative conditions (AIBN, air), oxaborole radical **4** has a chain path to closed-shell products, and boralactones are eventually produced in useful yields.

## Conclusions

We set out to generate the first NHC-boraallyl radicals by hydrogen abstraction reactions starting from (*E*)-alkenylboranes **3a–c**. However, the resulting sets of EPR data did not match either our expectations or DFT calculations. The breakthrough came when DFT calculations suggested that the expected boraallyl radicals would undergo a rapid 5-*endo* cyclization to form isomeric 1,2-oxaborole radicals **5a–c**. The DFT-computed EPR parameters of **5a–c** matched the spectra nicely, so in the end we observed the first 1,2-oxaborole radicals. Additional DFT calculations showed that stabilization of the oxaborole radicals by added  $\pi$ -conjugation is especially important to obtain a rapid and exothermic cyclization.

We then undertook preparative experiments in a search for stable products derived from the 1,2-oxaborole radicals.

Here we discovered that novel boralactones were formed when the precursor (*E*)-alkenylboranes were heated for a few hours with AIBN, Bu<sub>3</sub>SnH and air. These boralactones are the first examples of NHC complexes of borinic acid lactones. They are robust molecules that are stable to flash chromatography and storage in ambient lab conditions. Overall, these discoveries add to the increasingly rich chemistry of ligated boranes and their derived radicals.

## ASSOCIATED CONTENT

**Supporting Information.** Contains details of EPR experiments, calculations and preparative experiments along with copies of spectra of all new compounds. This material is available free of charge via the Internet at <http://pubs.acs.org>.

## AUTHOR INFORMATION

### Corresponding Authors

\* jcw@st-andrews.ac.uk; \* curran@pitt.edu .

### ORCID

Wen Dai: 0000-0002-9098-5215

Timothy R. McFadden: 0000-0002-8763-0376

Herbert A. Früchtl: 0000-0001-6647-4266

Dennis P. Curran: 0000-0001-9644-7728

John C. Walton: 0000-0003-2746-6276

## ACKNOWLEDGMENT

J.C.W. thanks EaStCHEM for financial support and D.P.C. thanks the US National Science Foundation. Computational support was provided through the EaStCHEM Research Computing Facility.

## REFERENCES

- (1) Curran, D. P.; Solovyev, A.; Makhlof Brahmi, M.; Fensterbank, L.; Malacria, M.; Lacôte, E. Synthesis and Reactions of N-Heterocyclic Carbene Boranes. *Angew. Chem. Int. Ed.* **2011**, *50*, 10294-10317.
- (2) a) Ren, S.-C.; Zhang, F.-L.; Qi, J.; Huang, Y.-S.; Xu, A.-Q.; Yan, H.-Y.; Wang, Y.-F. Radical Borylation/Cyclization Cascade of 1,6-Enynes for the Synthesis of Boron-handled Hetero- and Carbocycles. *J. Am. Chem. Soc.* **2017**, *139*, 6050-6053; b) Lalevéé, J.; Telitel, S.; Tehfe, M. A.; Fouassier, J. P.; Curran, D. P.; Lacôte, E. N-Heterocyclic Carbene Boranes Accelerate Type I Radical Photopolymerizations and Overcome Oxygen Inhibition. *Angew. Chem. Int. Ed.* **2012**, *51*, 5958-5961; c) Ueng, S.-H.; Solovyev, A.; Yuan, X.; Geib, S. J.; Fensterbank, L.; Lacôte, E.; Malacria, M.; Newcomb, M.; Walton, J. C.; Curran, D. P. N-Heterocyclic Carbene Boryl Radicals: A New Class of Boron-Centered Radical. *J. Am. Chem. Soc.* **2009**, *131*, 11256-11262.
- (3) a) Horn, M.; Mayr, H.; Lacôte, E.; Merling, E.; Deaner, J.; Wells, S.; McFadden, T.; Curran, D. P. N-Heterocyclic Carbene Boranes are Good Hydride Donors. *Org. Lett.* **2012**, *14*, 82-85; b) Prokofjevs, A.; Boussounière, A.; Li, L.; Bonin, H.; Lacôte, E.; Curran, D. P.; Vedejs, E. Borenum Ion Catalyzed Hydroboration of Alkenes with N-Heterocyclic Carbene-Boranes. *J. Am. Chem. Soc.* **2012**, *134*, 12281-12288.
- (4) a) Chen, D.; Zhang, X.; Qi, W.-Y.; Xu, B.; Xu, M.-H. Rhodium(II)-Catalyzed Asymmetric Carbene Insertion into B–H Bonds: Highly Enantioselective Access to Functionalized Organoborane. *J. Am. Chem. Soc.* **2015**, *137*, 5268-5271; b) Cheng, Q. Q.; Zhu, S. F.; Zhang, Y. Z.; Xie, X. L.; Zhou, Q. L. Copper-catalyzed B–H Bond Insertion Reaction: a Highly Efficient and Enantioselective C–B Bond-forming Reaction with Amine-borane and Phosphine-borane Adducts. *J. Am. Chem. Soc.* **2013**, *135*, 14094-14097; c) Li, X.; Curran, D. P. Insertion of Reactive Rhodium Carbenes into Boron–Hydrogen Bonds of Stable N-Heterocyclic Carbene Boranes. *J. Am. Chem. Soc.* **2013**, *135*, 12076-12081.



- (5) Hioe, J.; Karton, A.; Martin, J. M. L.; Zipse, H. Borane-Lewis Base Complexes as Homolytic Hydrogen Atom Donors. *Chem. Eur. J.* **2010**, *16*, 6861-6865.
- (6) a) Soleilhavou, M.; Bertrand, G. Cyclic (Alkyl)(Amino)Carbenes (CAACs): Stable Carbenes on the Rise. *Acc. Chem. Res.* **2015**, *48*, 256-266; b) de Oliveira Freitas, L. B.; Eisenberger, P.; Crudden, C. M. Mesoionic Carbene-Boranes. *Organometallics* **2013**, *32*, 6635-6638.
- (7) Walton, J. C.; Makhlof Brahmi, M.; Fensterbank, L.; Lacôte, E.; Malacria, M.; Chu, Q.; Ueng, S.-H.; Solovyev, A.; Curran, D. P. EPR Studies of the Generation, Structure, and Reactivity of N-Heterocyclic Carbene Borane Radicals. *J. Am. Chem. Soc.* **2010**, *132*, 2350-2358.
- (8) Walton, J. C.; Brahmi, M. M.; Monot, J.; Fensterbank, L.; Malacria, M.; Curran, D. P.; Lacôte, E. Electron Paramagnetic Resonance and Computational Studies of Radicals Derived from Boron-Substituted N-Heterocyclic Carbene Boranes. *J. Am. Chem. Soc.* **2011**, *133*, 10312-10321.
- (9) a) Silva-Valverde, M. F.; Schweyen, P.; Gisinger, D.; Bannenberg, T.; Freytag, M.; Kleeborg, C.; Tamm, M. N-Heterocyclic Carbene Stabilized Boryl Radicals. *Angew. Chem. Int. Ed.* **2017**, *56*, 1135-1140; b) Chiu, C. W.; Gabbai, F. P. A 9-Borylated Acridinyl Radical. *Angew. Chem. Int. Ed.* **2007**, *46*, 1723-1725.
- (10) McFadden, T. R.; Fang, C.; Geib, S. J.; Merling, E.; Liu, P.; Curran, D. P. Synthesis of Boriranes by Double Hydroboration Reactions of N-Heterocyclic Carbene Boranes and Dimethyl Acetylenedicarboxylate. *J. Am. Chem. Soc.* **2017**, *139*, 1726-1729.
- (11) Walton, J. C.; McFadden, T. R.; Curran, D. P. Generation and Structure of Unique Boriranyl Radicals. *J. Am. Chem. Soc.* **2017**, *139*, 16514-16517.
- (12) a) Barone, V.; Cossi, M. Quantum Calculation of Molecular Energies and Energy Gradients in Solution by a Conductor Solvent Model. *J. Phys. Chem. A*, **1998**, *102*, 1995-2001; b) Perdew, J. P.; Burke, K.; Ernzerhof, M. Generalized Gradient Approximation Made Simple. *Phys. Rev. Lett.* **1996**, *77*, 3865-3868; c) Grimme, S.; Anthony, J.; Ehrlich, S.; Krieg, H. A Consistent and Accurate *ab initio* Parametrization of Density Functional Dispersion Correction (DFT-D) for the 94 Elements H-Pu. *J. Chem. Phys.* **2010**, *132*, 154104/1-154104/19; d) Grimme, S.; Ehrlich, S.; Goerigk, L. Effect of the Damping Function in Dispersion Corrected Density Functional Theory. *J. Comp. Chem.* **2011**, *32*, 1456-1465; e) Weigend, F.; Ahlrichs, R. Balanced Basis Sets of Split Valence, Triple Zeta Valence and Quadruple Zeta Valence Quality for H to Rn: Design and Assessment of Accuracy. *Phys. Chem. Chem. Phys.* **2005**, *7*, 3297-3305; f) Barone, V. Structure, Magnetic Properties and Reactivities of Open-Shell Species from Density Functional and Self-Consistent Hybrid Methods. In *Recent Advances in Density Functional Methods, Part 1*; Chong, D. P. Ed.; World Scientific Publ. Co.: Singapore, 1996.
- (13) Gilmore, K.; Alabugin, I. V. Unusual Cyclizations. In *Encyclopedia of Radicals in Chemistry, Biology and Materials*; Chatgililoglu, C., Studer, A., Ed.; Wiley: NY, 2012; Vol. 1, p 1851-1894.
- (14) Mendenhall, G. D.; Protasiewicz, J. D.; Brown, C. E.; Ingold, K. U.; Luszyk, J. 5-Endo Closure of the 2-Formylbenzoyl Radical. *J. Am. Chem. Soc.* **1994**, *116*, 1718-1724.
- (15) For example, see: Zhang, L.; Cheng, J.; Carry, B.; Hou, Z. Catalytic Boracarboxylation of Alkynes with Diborane and Carbon Dioxide by an N-Heterocyclic Carbene Copper Catalyst. *J. Am. Chem. Soc.* **2012**, *134*, 14314-14317.
- (16) Two cyclic boracarbamates in the borinic acid oxidation state are described in: Barnett, B. R.; Moore, C. E.; Rheingold, A. L.; Figueroa, J. S. Frustrated Lewis Pair Behavior of Monomeric (Boryl)Iminomethanes Accessed from Isocyanide 1,1-Hydroboration. *Chem. Commun.* **2015**, *51*, 541-544.
- (17) a) Bohnke, J.; Braunschweig, H.; Dellermann, T.; Ewing, W. C.; Hammond, K.; Jimenez-Halla, J. O.; Kramer, T.; Mies, J. The Synthesis of B<sub>2</sub>(SIDip)<sub>2</sub> and its Reactivity between the Diboracumulenic and Diborynic Extremes. *Angew. Chem. Int. Ed.* **2015**, *54*, 13801-13805; b) Braunschweig, H.; Dellermann, T.; Dewhurst, R. D.; Ewing, W. C.; Hammond, K.; Jimenez-Halla, J. O. C.; Kramer, T.; Kruppenacher, I.; Mies, J.; Phukan, A. K.; Vargas, A. Metal-Free Binding and Coupling of Carbon Monoxide at a Boron-Boron Triple Bond. *Nat. Chem.* **2013**, *5*, 1025-1028.
- (18) De Vries, T. S.; Prokofjevs, A.; Vedejs, E. Cationic Tricoordinate Boron Intermediates: Borenum Chemistry from the Organic Perspective. *Chem. Rev.* **2012**, *112*, 4246-4282.
- (19) a) Larraufie, M.-H.; Malacria, M.; Courillon, C.; Ollivier, C.; Fensterbank, L.; Lacôte, E. Synthesis of Natural Quinazolinones and Some of Their Analogues through Radical Cascade Reactions Involving N-Acylcyanamides. *Tetrahedron* **2013**, *69*, 7699-7705; b) Beckwith, A. L. J.; Bowry, V. W.; Bowman, W. R.; Mann, E.; Parr, J.; Storey, J. M. D. The Mechanism of Bu<sub>3</sub>SnH-Mediated Homolytic Aromatic Substitution. *Angew. Chem. Int. Ed.* **2004**, *43*, 95-98; c) Josien, H.; Ko, S. B.; Bom, D.; Curran, D. P. A General Synthetic Approach to the (20S)-Camptothecin Family of Antitumor Agents by a Regiocontrolled Cascade Radical Cyclization of Aryl Isonitriles. *Chem. Eur. J.* **1998**, *4*, 67-83.
- (20) a) Hendry, D. G.; Schuetzle, D. Reaction of Hydroperoxy Radicals. Liquid-Phase Oxidation of 1,4-Hexadiene. *J. Am. Chem. Soc.* **1975**, *97*, 7123-7127; b) Howard, J. Reactions of Organic Peroxyl Radicals in Organic Solvents. In *Peroxy Radicals*; Alfassi, Z. B., Ed.; Wiley: Chichester, U.K. 1997; p 283-334.
- (21) Maillard, B.; Ingold, K. U.; Scaiano, J. C. Rate Constants for the Reactions of Free Radicals with Oxygen in Solution. *J. Am. Chem. Soc.* **1983**, *105*, 5095-5099.
- (22) Lowe, J. R.; Porter, N. A. Preparation of an Unsymmetrically Labeled Allylic Hydroperoxide and Study of Its Allylic Peroxyl Radical Rearrangement. *J. Am. Chem. Soc.* **1997**, *119*, 11534-11535.
- (23) a) Lacôte, E.; Curran, D. P.; Lalevé, J. NHC-Boranes: Air- and Water-tolerant Co-initiators for Type II Photopolymerizations. *Chimia* **2012**, *66*, 382-385; b) Tehfe, M.-A.; Monot, J.; Makhlof Brahmi, M.; Bonin-Dubarle, H.; Curran, D. P.; Malacria, M.; Fensterbank, L.; Lacôte, E.; Lalevé, J.; Fouassier, J.-P. N-Heterocyclic Carbene-Borane Radicals as Efficient Initiating Species of Photopolymerization Reactions under Air. *Polym. Chem.* **2011**, *2*, 625-631.
- (24) Nakamura, E.; Inubushi, T.; Aoki, S.; Machii, D. Aerobic Conversion of Organic Halides to Alcohols - An Oxygenative Radical Cyclization. *J. Am. Chem. Soc.* **1991**, *113*, 8980-8982.



---

TOC GRAPHIC

